BioMedical Engineering OnLine

BioMed Central

Research

Open Access

A mathematical model for electrical stimulation of a monolayer of cardiac cells

Ranjini Srinivasan and Bradley J Roth*

Address: Department of Physics, Oakland University, Rochester, Michigan 48309 USA

Email: Ranjini Srinivasan - sriniv33@msu.edu; Bradley J Roth* - roth@oakland.edu

* Corresponding author

Published: 27 January 2004

BioMedical Engineering OnLine 2004, **3**:1

Received: 08 October 2003

Accepted: 27 January 2004

This article is available from: http://www.biomedical-engineering-online.com/content/3/1/1

Abstract

Background: The goal of our study is to examine the effect of stimulating a two-dimensional sheet of myocardial cells. We assume that the stimulating electrode is located in a bath perfusing the tissue.

Methods: An equation governing the transmembrane potential, based on the continuity equation and Ohm's law, is solved numerically using a finite difference technique.

Results: The sheet is depolarized under the stimulating electrode and is hyperpolarized on each side of the electrode along the fiber axis.

Conclusions: The results are similar to those obtained previously by Sepulveda et al. (Biophys J, 55: 987–999, 1989) for stimulation of a two-dimensional sheet of tissue with no perfusing bath present.

Background

Pacemakers and defibrillators work by electrical stimulation of the heart. One way to learn more about electrical stimulation is to study very simple models, such as monolayers of cardiac cells [1]. An important factor during stimulation is anisotropy, which means the tissue has different electrical properties in different directions. Cardiac tissue is anisotropic in that the individual myocardial cells are cylindrical with a length greater than their width, and the cells align with each other to form fibers. This geometry makes the electrical conductivity of the tissue greater parallel to the fibers than perpendicular to them. Cell monolayers can be grown with any fiber geometry, making them a particularly attractive model system [2,3].

The goal of our study is to examine the effect of stimulating a two-dimensional sheet of cardiac tissue. We assume that the stimulating electrode is located in a bath perfusing the issue. In a previous study, Sepulveda et al. [4] simulated the electrical behavior of a two-dimensional sheet of tissue. They found that, when stimulated by a point cathode, the tissue near the cathode depolarized but adjacent regions hyperpolarized along the fiber direction. However, their model did not include a saline bath perfusing the tissue. Our study reexamines the results of Sepulveda et al., with particular emphasis on the effect of a perfusing bath.

The regions of depolarization and hyperpolarization (sometimes called "virtual electrodes") are important, because they are central to the mechanisms of make and break excitation [5,6]. In make excitation, wave fronts of electrical activity initiate following the start of the stimulus pulse, and propagate outwards from regions of depolarization. In break excitation, tissue hyperpolarizes and de-excites during the stimulus pulse. After the pulse, wave

fronts can propagate through this newly excitable tissue. Break wave fronts can initiate reentry [7,8], and are thought to be important during defibrillation of the heart [9,10]. These ideas can be illustrated online using a simple model of an excitable medium [11,12]. Our results suggest that researchers can study these important phenomena using cell monolayers.

Methods

The equation governing a two-dimensional sheet of tissue perfused by a three-dimensional bath is similar to the equation derived by Rattay for a one-dimensional nerve axon [13]. The tissue obeys the conservation of current,

$$\frac{\partial J_{ix}}{\partial x} + \frac{\partial J_{iy}}{\partial y} = -\beta J_m, \qquad (1)$$

where β is the ratio of membrane surface area to tissue volume, J_m is the membrane current density, and J_{ix} and J_{iy} represent x and y components of the intracellular current density. Ohm's Law gives

$$J_{ix} = -\sigma_{ix} \frac{\partial V_i}{\partial x}, \qquad (2)$$

$$J_{iy} = -\sigma_{iy} \frac{\partial V_i}{\partial y}, \qquad (3)$$

$$J_m = G_m V_m, \qquad (4)$$

where V_i is the intracellular potential, V_m is the transmembrane potential, G_m is membrane conductivity per unit area, and σ_{ix} and σ_{iy} are the intracellular conductivities parallel to (x) and perpendicular to (y) the fiber axis. Substituting Eqs. (2), (3), and (4) into Eq. (1), and letting $V_i = V_m + V_e$, we find that

$$\lambda_x^2 \frac{\partial^2 V_m}{\partial x^2} + \lambda_y^2 \frac{\partial^2 V_m}{\partial y^2} - V_m = -\lambda_x^2 \frac{\partial^2 V_e}{\partial x^2} - \lambda_y^2 \frac{\partial^2 V_e}{\partial y^2}, \qquad (5)$$

where λ_x and λ_y are defined as

$$\lambda_x = \sqrt{\frac{\sigma_{ix}}{\beta G_m}} \qquad (6)$$

$$\lambda_y = \sqrt{\frac{\sigma_{iy}}{\beta G_m}}. \qquad (7)$$

In order to solve Eq. (5), we must first determine the extracellular potential, V_e. We assume that V_e is from a point electrode in an infinite, homogeneous bath

$$Ve = \frac{I}{4\pi\sigma_e r}, \qquad (8)$$

where $r = \sqrt{x^2 + y^2 + (z-d)^2}$, σ_e is the conductivity of the bath, I is the stimulus current, and d is the distance from the tissue sheet ($z = 0$) to the electrode.

We discretize Eq. (5) using a finite difference formula, and solve it using a relaxation method. The number of nodes in each direction is 100, the space step is 0.2 mm (implying a tissue size of 20 × 20 mm), σ_e is 1 S/m, I is 1 mA, and d is 1 mm.

Results

Figure 1 shows $V_m(x,y)$ for isotropic tissue with $\lambda_x = \lambda_y = 1$ mm. The electrode is located above the center of the plot. The color indicates the value of the transmembrane potential, with yellow indicating depolarization, purple rest, and blue hyperpolarization. The tissue is depolarized by 30 mV directly under the electrode. The region of depolarization is surrounded by halo of weak, diffuse hyperpolarization with a peak value of -0.6 mV, which is difficult to distinguish from resting tissue using the color scale in Fig. 1. Isocontours of the transmembrane potential are concentric circles, implying that V_m is independent of direction.

Figure 2 shows $V_m(x,y)$ for $\lambda_x = 1$ mm and $\lambda_y = 0$ mm. The x direction (fiber axis) is horizontal. Like in Fig. 1, the tissue is depolarized under the electrode (20 mV). However, hyperpolarization exists to the left and right of the electrode, with a peak hyperpolarization of -3.8 mV. This simulation corresponds to no coupling of cells in the transverse direction, as would be appropriate for a nerve.

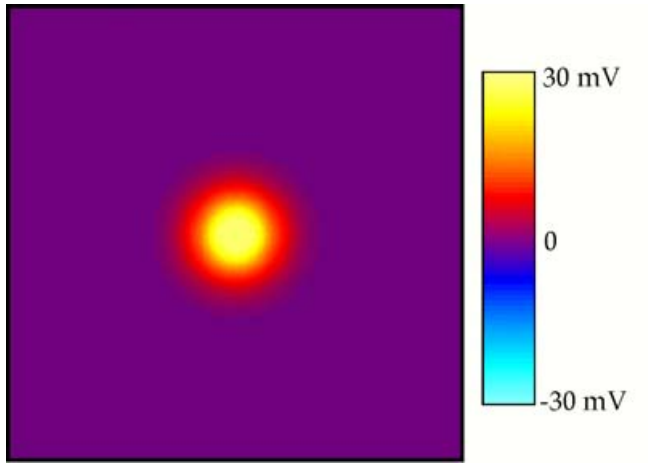

Figure 1
The transmembrane potential as a function of x and y. The electrode is above the center of the sheet, and the x direction is horizontal. Only the central 10 mm × 10 mm is displayed. $\lambda_x = \lambda_y = 1$ mm.

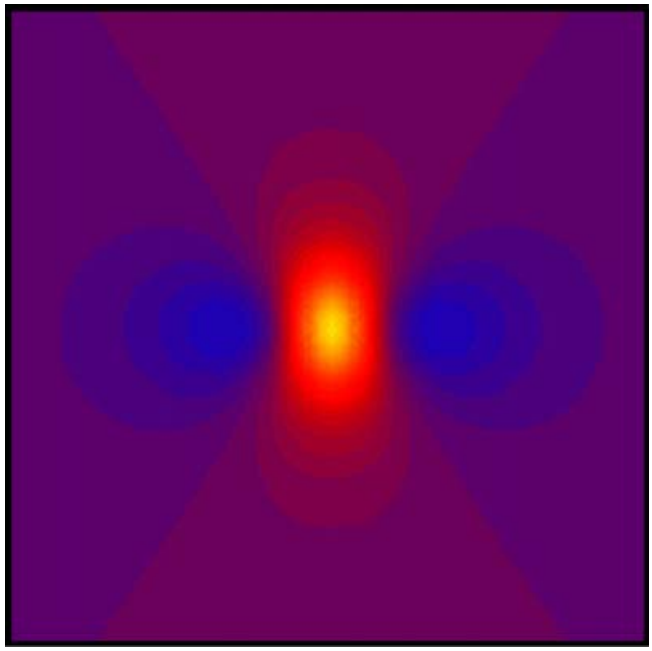

Figure 2
The transmembrane potential as a function of x and y. The electrode is above the center of the sheet, and the x direction is horizontal. Only the central 10 mm × 10 mm is displayed. The color scale is the same as in Fig. 1. λ_x = 1 mm and λ_y = 0.

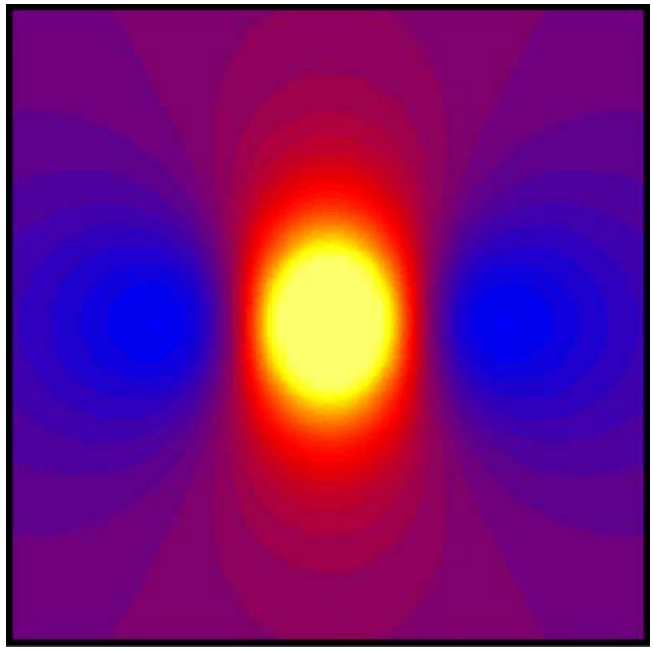

Figure 3
The transmembrane potential as a function of x and y. The electrode is above the center of the sheet, and the x direction is horizontal. Only the central 10 mm × 10 mm is displayed. The color scale is the same as in Fig. 1. λ_x = 1 mm and λ_y = 0.4 mm.

Figure 3 shows V_m when λ_x = 1 mm and λ_y = 0.4 mm. The distribution of V_m is qualitatively similar to that in Fig. 2, with depolarization under the electrode (23 mV) and hyperpolarization on each side of the electrode along the fiber direction (-2.5 mV). This simulation uses parameters typical of normal cardiac tissue [14].

The transmembrane potential depends sensitively on the height of the electrode above the plane of the tissue sheet, d. Figure 4 shows the peak depolarization as a function of d for the case of normal cardiac tissue. The dashed line has a slope of negative two on this log-log plot, and corresponds to a $1/d^2$ fall off of the depolarization. This figure explains why the stimulation threshold changes when an electrode is moved away from the monolayer.

To test our numerical accuracy, we decrease the space step size to 0.05 mm and increase the number of nodes to 400 × 400 while keeping the tissue size fixed, and find that the maximum and minimum values of V_m vary by about 1%. In another simulation, we keep the space step constant at 0.2 mm and increase the number of nodes to 400 × 400, thereby increasing the size of the tissue sheet to 80 mm × 80 mm. The maximum and minimum values of V_m vary by 3%.

Discussion

Figure 3 is our primary result. The transmembrane potential distribution is qualitatively similar to that calculated in a two-dimensional sheet by Sepulveda et al. [4]. In particular, both calculations predict adjacent regions of depolarization and hyperpolarization near the stimulating electrode. The main difference between our calculation and theirs is the presence of a perfusing bath in our model. We therefore conclude that the qualitative distribution of transmembrane potential is insensitive to the perfusing bath. This result is important, because the adjacent regions of depolarization and hyperpolarization were responsible for break excitation and reentry induction. Experimenters should be able to study these phenomena using superfused cell monolayers.

Our results are quantitatively different than those of Sepulveda et al. [4]. For instance, the peak depolarization in their calculation was infinite because they used a point electrode embedded in the sheet of tissue. We do not predict an infinite depolarization because our electrode is a

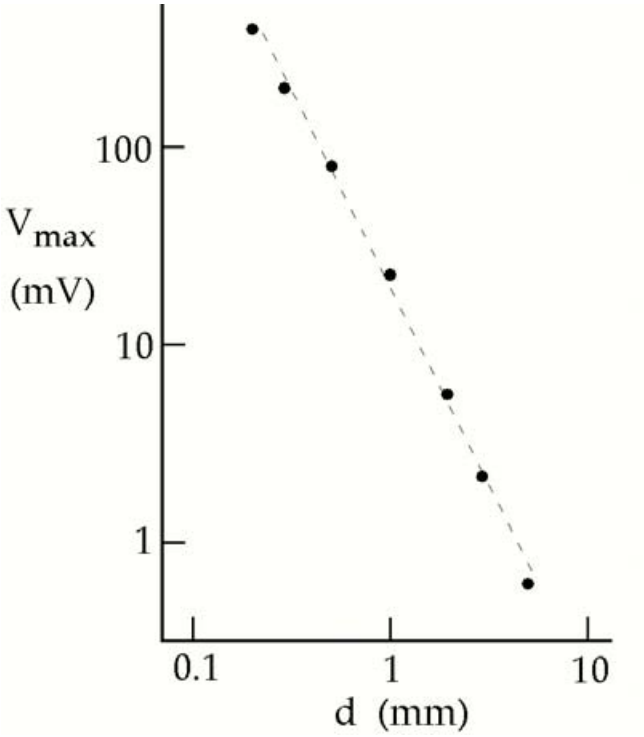

Figure 4
The peak depolarization under the electrode, as a function of distance from the electrode to the tissue sheet, *d*, for λ_x = 1 mm and λ_y = 0.4 mm. The dashed line has a slope of -2 in this log-log plot.

distance *d* from the tissue sheet. One advantage of our calculation over Sepulveda et al.'s is that our stimulus current is expressed in milliamps whereas theirs is in meters-milliamps, as required by their fully two-dimensional model.

Our simulations are similar to those by Latimer and Roth [15], in which an electrode in an adjacent perfusing bath stimulated a three-dimensional slab of cardiac tissue. The main difference between our calculation and theirs is that their three-dimensional geometry implied certain boundary conditions on the potential and potential gradient at the tissue surface. In a three-dimensional model, a potential gradient can exist in the z-direction. Because the intracellular space is sealed, such an electric field polarizes the tissue within a few length constants of the surface [16]. This boundary effect is not present in our model because the tissue sheet is two-dimensional and therefore cannot have a transmembrane potential gradient in the z-direction.

Our results in Fig. 2 are almost identical to the results found by Rattay when studying the stimulation of nerve axons. Rattay referred to the source term in his partial differential equation for V_m as the "activating function" [13]. Sobie et al. [17] have analyzed electrical stimulation of cardiac tissue using a similar concept. If we use this terminology, the expression on the right-hand-side of Eq. (5),

$$\lambda_x{}^2 \frac{\partial^2 V_e}{\partial x^2} + \lambda_y{}^2 \frac{\partial^2 V_e}{\partial y^2}, \qquad (9)$$

is the activating function.

One approximation that is implicit in our analysis is that the cell monolayer itself does not significantly perturb the extracellular potential distribution, so we can use Eq. (8) for V_e. Rattay used a similar approximation for his analysis of nerve stimulation [13]. If the monolayer is grown on glass or any other insulating substrate, as is commonly the case, then the substrate will perturb the extracellular potential. For a monolayer grown directly on the surface of the substrate, image analysis [18] implies that the extracellular potential experienced by the monolayer will still be equal to the expression given in Eq. (8), except for an additional factor of two. To prove this surprising result, consider the potential produced by two current sources in an unbounded bath, one at x = y = 0 and z = d, and the other at x = y = 0 and z = -d. Let both sources have the same strength and polarity. The resulting potential distribution will be a generalization of Eq. (8)

$$V_e = \frac{I}{4\pi\sigma_e}\left[\frac{1}{\sqrt{x^2+y^2+(z-d)^2}} + \frac{1}{\sqrt{x^2+y^2+(z+d)^2}}\right]. \qquad (10)$$

This potential distribution obeys Poisson's equation for z > 0, and has zero derivative in the z-direction at the surface z = 0. Because of the uniqueness of the solution to Poisson's equation, Eq. (10) must therefore be the potential produced by a point current source a distance *d* from an insulating surface. Throughout the bath, Eq. (10) predicts a different potential than does Eq. (8). This difference can be thought of as arising from secondary sources at the insulating boundary, which are correctly accounted for by the image method [18]. However, at the surface z = 0 Eqs. (8) and (10) give identical results, except for a factor of two. This useful result means that a monolayer grown on an insulating surface will experience the same activating function as a monolayer grown in an infinite bath, except that the activating function is twice as large.

One interesting conclusion of our calculation is that the magnitude of the induced transmembrane potential varies inversely with the conductivity of the perfusing bath. This conclusion is true when the stimulating electrode is attached to a current source, as we assumed in our calculation (in our model, the stimulus current *I* is specified independently of the bath conductivity, the distance

d, or any other parameters). If the conductivity of the bath increases, the magnitude of the induced polarization decreases (voltage drops are smaller for a given current), but the spatial distribution of V_m is unchanged.

In conclusion, the transmembrane potential induced when stimulating a monolayer of cardiac cells is similar to the transmembrane potential distribution predicted by Sepulveda et al. [4] when analyzing stimulation of a two-dimensional sheet of cardiac tissue. The presence of a perfusing bath above the sheet changes the quantitative value of V_m, but has little effect on its qualitative spatial distribution. Therefore, cell monolayers represent a well-controlled system which experimentalists could use to study break stimulation and the induction of reentry.

Acknowledgements

This research was supported by the National Institute of Health (RO1 HL57207).

For more information please contact BJ Roth (http://www.Oakland.edu/~roth

References

1. Fast VG, Cheek ER: **Optical mapping of arrhythmias induced by strong defibrillation shocks in myocyte cultures.** *Circ Res* 2002, **90:**664-670.
2. Tung L, Kleber AG: **Virtual sources associated with linear and curved strands of cardiac cells.** *Am J Physiol Health Circ Physiol* 2000, **279:**1579-1590.
3. Fast VG, Kleber AG: **Anisotropic conduction in monolayers of neonatal rat heart cells cultured on collagen substrate.** *Circ Res* 1994, **75:**591-595.
4. Sepulveda NG, Roth BJ, Wikswo JP Jr: **Current injection into a two-dimensional anisotropic biodomain.** *Biophys J* 1989, **55:**987-999.
5. Roth BJ: **A mathematical model of make and break electrical stimulation of cardiac tissue by a unipolar anode or cathode.** *IEEE Trans Biomed Eng* 1995, **42:**1174-1184.
6. Wikswo JP Jr, Lin S-F, Abbas RA: **Virtual electrodes in cardiac tissue: A common mechanism for anodal and cathodal stimulation.** *Biophys J* 1995, **69:**2195-2210.
7. Roth BJ: **Nonsustained reentry following successive stimulation of cardiac tissue through a unipolar electrode.** *J Cardiovasc Electrophysiol* 1997, **8:**768-778.
8. Lin S-F, Roth BJ, Wikswo JP Jr: **Quatrefoil reentry in myocardium: An optical imaging study of the induction mechanism.** *J Cardiovasc Electrophysiol* 1999, **10:**574-586.
9. Efimov IR, Gray RA, Roth BJ: **Virtual electrodes and de-excitation: new insights into fibrillation induction and defibrillation.** *J Cardiovasc Electrophysiol* 2000, **11:**339-353.
10. Trayanova N: **Concepts of ventricular defibrillation.** *Phil Trans R Soc Lond A* 2001, **359:**1327-1337.
11. Roth BJ: **Virtual electrodes made simple: A cellular excitable medium modified for strong electrical stimuli.** *The Online Journal of Cardiology* [http://sprojects.mmi.mcgill.ca/heart/pages/rot/rothom.html].
12. Winfree AT: **When Time Breaks Down.** *Princeton University Press, Princeton, NJ*; 1987.
13. Rattay F: **Analysis of models for extracellular fiber stimulation.** *IEEE Trans Biomed Eng* 1989, **36:**676-682.
14. Roth BJ: **Electrical conductivity values used with the bidomain model of cardiac tissue.** *IEEE Trans Biomed Eng* 1997, **44:**326-328.
15. Latimer DC, Roth BJ: **Electrical stimulation of cardiac tissue by a bipolar electrode in a conductive bath.** *IEEE Trans Biomed Eng* 1998, **45:**1449-1458.
16. Weidmann S: **Electrical constants of trabecular muscle from mammalian heart.** *J Physiol* 1970, **210:**1041-1054.
17. Sobie EA, Susil RC, Tung L: **A generalized activating function for predicting virtual electrodes in cardiac tissue.** *Biophys J* 1997, **73:**1410-1428.
18. Jackson JD: **Classical Electrodynamics.** 3rd edition. *Wiley, New York*; 1999.